

Oligopeptide Delivery Carrier for Osteoclast Precursors

Bo Chi,[†] So Jeong Park,[‡] Min Hee Park,[†] Soo Young Lee,^{*,‡} and Byeongmoon Jeong^{*,†}

Department of Chemistry and Nano Science and Division of Life and Pharmaceutical Sciences, Department of Bioinspired Science, Ewha Womans University, Seoul, Korea. Received February 2, 2010; Revised Manuscript Received June 2, 2010

Dendritic amine and guanidinium group-modified nanoparticles were investigated for the delivery of model peptide drug into primary osteoclast precursor cells (bone marrow macrophages; BMMs). The model peptide drug was encapsulated into the nanoparticle by dropping the drug/carrier dissolved in dimethylsulfoxide/methylene chloride cosolvent into water containing poly(vinyl alcohol) as a stabilizer. Flow cytometry and spectrofluorimetry analysis indicated that the model drug itself was not taken up by the BMMs; however, nanoparticle systems underwent significant cellular uptake. In particular, guanidinium group-modified nanoparticles were taken up more efficiently than amine group-modified ones. Cell viability studies showed that both amine and guanidinium group-modified nanoparticles exhibited no significant cytotoxicity up to 100 $\mu\text{g/mL}$ against the cells.

INTRODUCTION

Cellular communications between osteoblasts and osteoclasts are the basic mechanism of bone homeostasis. Increased activity of osteoclasts relative to osteoblasts leads to diseases such as osteoporosis, periodontitis, and arthritis (1, 2). The inhibition of differentiation from precursor cells (bone marrow macrophages; BMMs) into osteoclasts was suggested to be a promising therapeutic treatment for such diseases (3). We have been developing oligopeptides that inhibit osteoclast differentiation (4). However, they need a carrier system to deliver the drug into the BMMs; otherwise, it cannot enter the cells due to the large size and charge of the drug.

Plasma membrane serves as the protective barrier against extraneous molecules into living cells. To overcome the cell membrane barriers, cell penetrating peptides (CPPs) have been extensively investigated for the plasmid DNA, oligonucleotide, si-RNA, peptide–nucleic acid (PNA), proteins, liposomes, and iron nanoparticles (5, 6). TAT, penetratin, model amphipathic peptide (MAP), transportan, vascular endothelial cadherin derived CPP (pVEC), pISL derived from the homeodomain of the rat transcription factor Islet-1, oligoarginine, KETWWETW-WTEWSQPKKRRK (Pep-1), and MANLGYWLLALFVT-MWTDVGLCKRKP (PrP^c) are typical examples of the CPPs. The structural characteristics of these CPPs are positively charged amino acids such as lysine or arginine in the peptide sequence. In particular, guanidinium moieties are intensively studied by Futaka and Wender, focusing on the dependence of molecular weight of oligoarginine, topological variation into linear and dendritic oligoarginine (7–11). The optimal number of Arg with 8–9 is critical, because it determines the toxicity, translocation ability of the conjugated drug, and cost of the system (9, 10).

In this research, we designed a series of dendritic amine and guanidinium modified molecules, where a hydrophobic stearyl group is connected to the amine or guanidinium groups, and oligophenylalanine is used as a connecting moiety to give structural rigidity to the system (Figure 1). The hydrophobic

stearyl group is used to encapsulate the hydrophobic model oligopeptide drug, an FITC conjugated-Ile-Ile-Leu-Ala-Val-Tyr (FITC-IILAVY). Internalization of the model oligopeptide drug into the BMMs was investigated using a series of these nanoparticles carriers.

EXPERIMENTAL PROCEDURES

Materials. FITC-IILAVY was obtained from Pepton (Korea). *N*-Carboxyanhydride of DL-phenylalanine (DL-Phe-NCA) was purchased from M&H laboratories (Korea). α,ϵ -Di-*tert*-butyloxycarbonyl-L-lysine (α,ϵ -diboc-Lys) was purchased from Shanghai GL Biochem Ltd. (China). Stearylamine and 1-ethyl-3-(3-dimethyl aminopropyl) carbodiimide (EDC) were purchased from TCI (Japan). *N*-Hydroxysuccinimide (NHS), 4-guandibutyric acid (GBA), dimethylsulfoxide (DMSO), paraformaldehyde, and anhydrous *N,N*-dimethyl formamide (DMF) were purchased from Sigma (America). Trifluoroacetic acid (TFA) and 4-morpholine ethane sulfonic acid (MES) were purchased from Sigma (America) and used as received.

Synthesis of SF-A1. Stearylamine in anhydrous DMF (5.3 mL, 1.0 M) was added to a DL-Phe-NCA 3.06 g (16.0 mmol) solution dissolved in anhydrous DMF (20 mL), and the reaction was stirred 4 days at 40 °C under N₂ protection (12). The mixtures were precipitated in diethyl ether, and the precipitate was washed throughout with diethyl ether. The product was dried in vacuo.

[M-Na⁺]: 733.7 (calc. 734.0). ¹H NMR (CF₃COOD): δ (ppm) stearylamine (CH_2 -) = 0.7–1.0; δ stearylamine ($-\text{CH}_2-$) = 1.0–1.5; δ stearylamine ($-\text{CH}_2\text{NH}-$) = 3.0–3.1; DL-phenylalanine ($-\text{CH}_2-$) = 3.1–3.4; δ DL-phenylalanine ($-\text{COCH}(\text{CH}_2\text{C}_6\text{H}_5)-$) = 4.6–5.0; δ DL-phenylalanine ($-\text{C}_6\text{H}_5$) = 6.8–7.4.

Synthesis of SF-G1. EDC (0.57 g, 3.0 mmol) and NHS (0.34 g, 3.0 mmol) were added to the GBA (0.43 g, 3.0 mmol) that was dissolved in MES buffer (pH = 5.5, 10 mL). The reaction mixtures were stirred for 4 h. To couple the amino group of the SF-A1 and carboxylic acid group of GBA, SF-A1 (1.51 g, 1.80 mmol) dissolved in DMF (30 mL) was slowly injected to the reaction mixtures at 0 °C (13). The reaction was stirred at room temperature for 48 h. The reaction mixtures were precipitated into an excess amount of diethyl ether. The precipitate was filtered and washed with diethyl ether three times. After being dried in vacuo, the product was suspended in 20 mL of deionized water and dialyzed using cellulose

* To whom correspondence should be addressed. B. Jong: Fax 82232772384; Tel 82232773411; E-mail bjeong@ewha.ac.kr. S. Lee: Fax 82232773760; Tel 82232773770; E-mail leesy@ewha.ac.kr.

[†] Department of Chemistry and Nano Science.

[‡] Division of Life and Pharmaceutical Sciences.

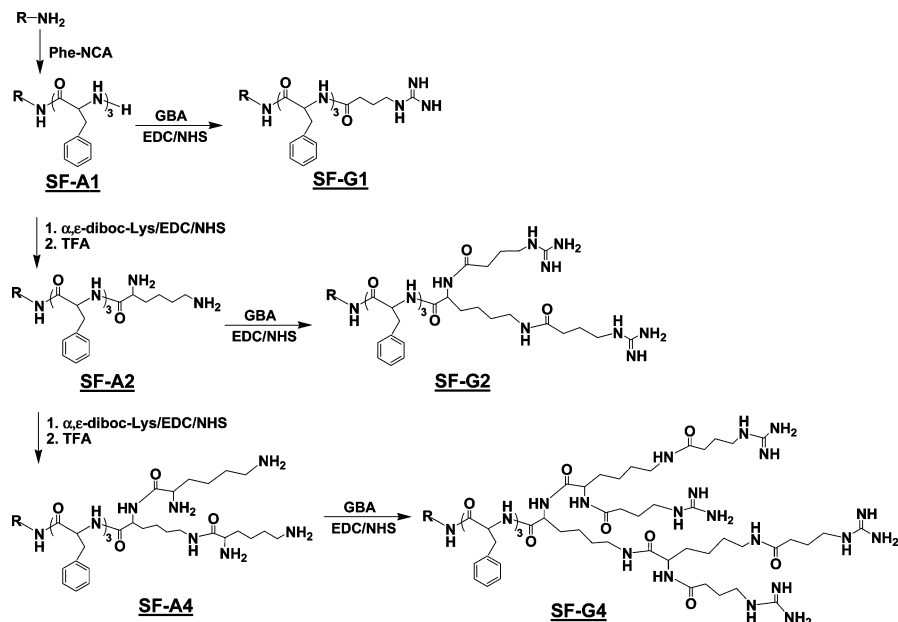


Figure 1. Synthetic scheme of carriers. R is stearyl (C_{17}) group. $n \approx 3$.

membrane (MWCO 500 Da) in deionized water for 24 h. The final product was lyophilized in a powder form.

MALDI-TOF Mass spectra [M-H⁺]: 839.0 (calc. 839.2). ¹H NMR (CF_3COOD): δ (ppm) stearylamine (CH_3 -) = 0.7–1.0; δ stearylamine ($-CH_2$ -) = 1.0–1.5; δ GBA ($-OCCH_2CH_2CH_2NH$ -) = 1.8–2.0; δ stearylamine ($-CH_2NH$ -) = 3.0–3.1; δ DL-phenylalanine ($-CH_2$ -) = 3.1–3.4; δ GBA ($-CH_2NHC(=NH)NH_2$) = 3.3–3.4; δ DL-phenylalanine ($-COCH(CH_2C_6H_5)$ -) = 4.6–5.0; δ DL-phenylalanine ($-C_6H_5$) = 6.8–7.4.

Synthesis of SF-A2. α, ϵ -Diboc-Lys (2.41 g, 7.0 mmol) was dissolved in MES buffer (pH = 5.5, 10 mL), and then EDC (1.34 g, 7.0 mmol) and NHS (0.81 g, 7.0 mmol) were added to the solution, and the mixture was stirred for 4 h. A solution of SF-A1 (4.00 g, 4.8 mmol) in DMF 30 mL was injected into the mixture at 0 °C. The reaction was stirred at room temperature for 48 h. The protective *t*-butoxycarbonyl groups were removed by TFA. The SF-A1-diboc-lysine (4.34 g, 4.2 mmol) was stirred in a mixed solution of TFA (10 mL) and anhydrous dichloromethane (20 mL) at 0 °C for 3 h. After the solvent was partially evaporated under reduced pressure, an excess amount of diethyl ether was added to precipitate SF-A2. The precipitate was filtered and washed with diethyl ether three times. After being dried in vacuo, the product was dissolved in 20 mL deionized water and dialyzed using cellulose membrane (MWCO 500 Da) in deionized water for 24 h. The final product was collected by lyophilization.

MALDI-TOF Mass spectra [M-H⁺]: 839.9 (calc. 839.2). ¹H NMR (CF_3COOD): δ (ppm) stearylamine (CH_3 -) = 0.7–0.9; δ stearylamine ($-CH_2$ -) = 1.0–1.5; δ lysine ($-COCH(CH_2CH_2CH_2CH_2(NH_2))$) = 1.6–1.7; δ lysine ($-COCH(CH_2CH_2CH_2CH_2(NH_2))$) = 1.8–2.0; δ lysine ($-COCH(CH_2CH_2CH_2CH_2(NH_2))$) = 2.8–3.2; δ stearylamine ($-CH_2NH$ -) = 3.0–3.1; δ DL-phenylalanine ($-CH_2$ -) = 3.1–3.4; δ lysine ($-COCH(CH_2CH_2CH_2CH_2(NH_2))(NH_2)$); and DL-phenylalanine ($-COCH(CH_2C_6H_5)$ -) = 4.6–5.0; δ DL-phenylalanine ($-C_6H_5$) = 6.8–7.4.

Synthesis of SF-G2. GBA (1.30 g, 9.0 mmol) was dissolved in MES buffer (10 mL at pH = 5.5). EDC (1.77 g, 9.0 mmol) and NHS (1.0 g, 9.0 mmol) were added to the solution, and the mixtures were stirred for 4 h at room temperature. SF-A2 (3.15 g, 3.8 mmol) in DMF (30 mL) was injected into the mixture at 0 °C, and the reaction mixtures were stirred at room temperature for 48 h. The reaction mixtures were poured into an excess

amount of diethyl ether to precipitate the product. The precipitate was filtered and washed with diethyl ether three times. After the residual solvent was removed in vacuo, the product was redissolved in 20 mL deionized water and dialyzed using cellulose membrane (MWCO 500 Da) in deionized water for 24 h. The final product was collected by lyophilization.

MALDI-TOF Mass spectra [M-H⁺]: 1094.0 (calc. 1093.5). ¹H NMR (CF_3COOD): δ (ppm) stearylamine (CH_3 -) = 0.7–0.9; δ stearylamine ($-CH_2$ -) = 1.0–1.5; δ lysine ($-COCH(CH_2CH_2CH_2CH_2(NH_2))$) = 1.6–1.7; δ lysine ($-COCH(CH_2CH_2CH_2CH_2(NH_2))$) = 1.8–2.0; δ stearylamine ($-CH_2NH$ -) = 3.0–3.1; δ lysine ($-COCH(CH_2CH_2CH_2CH_2(NH_2))$) = 3.0–3.2; δ DL-phenylalanine ($-CH_2$ -) = 3.1–3.4; δ GBA ($-CH_2NHC(=NH)NH_2$) = 3.3–3.4; δ lysine ($-COCH(CH_2CH_2CH_2CH_2(NH_2))(NH_2)$), and DL-phenylalanine ($-COCH(CH_2C_6H_5)$ -) = 4.7–5.0; δ DL-phenylalanine ($-C_6H_5$) = 7.0–7.4.

Synthesis of SF-A4. α, ϵ -Diboc-Lys (4.83 g, 14.0 mmol) was dissolved in MES buffer (30 mL, pH = 5.5). EDC (2.70 g, 14.1 mmol) and NHS (1.65 g, 14.0 mmol) were added to the solution, and the mixtures were stirred for 4 h. SF-A2 (3.15 g, 3.8 mmol) dissolved in DMF (30 mL) was injected to the mixture at 0 °C, and the reaction mixtures were stirred at room temperature for 48 h. An excess amount of diethyl ether was added to precipitate the SF-A2- α, ϵ -diboc-Lys. The precipitate was filtered and washed with diethyl ether three times. After drying the product in vacuo, SF-A2- α, ϵ -diboc-Lys (5.14 g, 3.4 mmol) was stirred in a mixed solution of TFA (10 mL) and anhydrous dichloromethane (20 mL) at 0 °C for 3 h. After the solvent was partially evaporated under reduced pressure, an excess amount of diethyl ether was added to precipitate the product. The precipitate was filtered and washed with diethyl ether three times. After the residual solvent was removed in vacuo, the product was redissolved in 20 mL deionized water and dialyzed using a cellulose membrane (MWCO 500 Da) in deionized water for 24 h. The final product was collected by lyophilization.

MALDI-TOF Mass spectra [M-Na⁺]: 1118.0 (calc. 1118.6). ¹H NMR (CF_3COOD): δ (ppm) stearylamine (CH_3 -) = 0.7–0.9; δ stearylamine ($-CH_2$ -) = 1.0–1.5; δ lysine ($-COCH(CH_2CH_2CH_2CH_2(NH_2))$) = 1.6–1.7; δ lysine ($-COCH(CH_2CH_2CH_2CH_2(NH_2))$) = 1.8–2.0; δ lysine ($-COCH(CH_2CH_2CH_2CH_2(NH_2))$) = 2.8–3.2; δ stearylamine ($-CH_2NH$ -)

= 3.0–3.1; δ DL-phenylalanine ($-CH_2-$) = 3.1–3.4; δ lysine ($-\text{COCH}(\text{CH}_2\text{CH}_2\text{CH}_2\text{CH}_2\text{NH}_2)(\text{NH}_2)$); and DL-phenylalanine ($-\text{COCH}(\text{CH}_2\text{C}_6\text{H}_5)-$) = 4.6–5.0; δ DL-phenylalanine ($-C_6H_5$) = 6.8–7.4.

Synthesis of SF-G4. GBA (2.63 g, 18 mmol) was dissolved in MES buffer (pH = 5.5; 10 mL). EDC (3.62 g, 18.9 mmol) and NHS (2.10 g, 18.3 mmol) were added to the solution, and the mixtures were stirred for 4 h. SF-A4 (4.00 g, 3.7 mmol) dissolved in DMF (30 mL) was injected to the mixture at 0 °C, and the reaction mixtures were stirred at room temperature for 48 h. The reaction mixtures were precipitated into an excess amount of diethyl ether. The precipitate was filtered and washed with diethyl ether three times. After the residual solvent was removed in vacuo, the product was redissolved in 20 mL deionized water and dialyzed using cellulose membrane (MWCO 1000 Da) in deionized water for 24 h. The final product was collected by lyophilization.

MALDI-TOF Mass spectra [M-H⁺]: 1608.6 (calc. 1608.1). ¹H NMR (CF₃COOD): δ (ppm) stearylamine (CH_3-) = 0.7–0.1.0; δ stearylamine ($-CH_2-$) = 1.0–1.5; δ lysine ($-\text{COCH}(\text{CH}_2\text{CH}_2\text{CH}_2\text{CH}_2\text{NH}_2)-$) = 1.6–1.7; δ lysine ($-\text{COCH}(\text{CH}_2\text{CH}_2\text{CH}_2\text{CH}_2\text{NH}_2)-$), and GBA ($-\text{OCCH}_2\text{CH}_2\text{CH}_2\text{NH}-$) = 1.7–2.0; δ stearylamine ($-CH_2\text{NH}-$) = 3.0–3.1; δ DL-phenylalanine ($-CH_2-$) = 3.1–3.4; δ GBA ($-CH_2\text{NHC}(=\text{NH})\text{NH}-$) = 3.3–3.4; δ lysine ($-\text{COCH}(\text{CH}_2\text{CH}_2\text{CH}_2\text{CH}_2\text{NH}_2)(\text{NH}_2)$) = 4.5–4.8; δ DL-phenylalanine ($-\text{COCH}(\text{CH}_2\text{C}_6\text{H}_5)-$) = 4.7–5.0; δ DL-phenylalanine ($-C_6H_5$) = 6.8–7.4.

Preparation of Nanoparticles. FITC-IILAVY loaded nanoparticles were prepared by the emulsion–solvent evaporation technique (14). Briefly, the carrier (10 mg) dissolved in methylene chloride (2 mL) was mixed with FITC-IILAVY (100 μg) dissolved in 500 μL DMSO. The mixture was slowly dropped into poly(vinyl alcohol) aqueous solution (50 mL; 1.0% w/v) while stirring at 3200 rpm. The pre-emulsion equilibrated in an ice bath was sonicated for 10 min by using a 750 W high-intensity ultrasonic processor (VCX 750, Sonics and Materials Inc., USA) operating at 20 kHz. The organic solvent was then evaporated under gentle agitation (800 rpm) over 12 h at room temperature. The resulting nanoparticles were dialyzed using cellulose membrane (MWCO 3500 Da) in an excess amount of water for 24 h and freeze–dried for 48 h to a powder form.

Particle Size Analysis. Size and size distribution of the drug-loaded nanoparticles were measured by the particle size analyzer (Zetasizer NanoZS2000; Malven Instrument, UK) based on quasi-elastic light scattering. The nanoparticles were resuspended at a 1.0 mg/mL (wt./v) concentration in deionized water. Then, size and size distribution of the nanoparticles were measured at room temperature ($n = 3$).

Determination of Drug Encapsulation Efficiency and Drug Loading Content. The FITC-IILAVY loaded in the nanoparticles was analyzed by HPLC (Waters LC). Briefly, the drug loaded nanoparticles (1.0 mg) were dissolved in 1.0 mL DMSO. A Waters Nova-Pak C18 (3.9ch150 mm, 4 μm) column and UV/vis detector operating at 220 nm were used to analyze the drug content in the nanoparticle. The flow rate of the mobile phase (acetonitrile/water (50/50 by volume)) was 1.0 mL/min. The drug encapsulation efficiency is defined by the amount of drug encapsulated in the nanoparticle relative to the initial amount of drug. The drug loading content is the ratio of the amount of drug to nanoparticles.

Cell Culture. BMMs were obtained from the femur of 5 week old C57BL/6 mice. BMMs were flushed out of the bone marrow cavity. BMMs were suspended for 3 days in a α -minimal essential medium (α -MEM) (GIBCO-BRL, Grand Island, NY) supplemented with 10% heat-inactivated fetal bovine serum, 100 units/mL penicillin, 100 $\mu\text{g}/\text{mL}$ streptomycin (GIBCO), and 30

ng/mL recombinant human macrophage-colony stimulating factor (rhM-CSF) (R&D system, Minneapolis, MN).

Fluorescence Image Assay. BMMs were incubated in α -MEM containing drug-loaded nanoparticles for 4 h. The cells were washed twice with phosphate buffered saline (PBS). Culture dishes were transferred to a Zeiss Axiovert 200 microscope (Carl Zeiss, Oberkochen, Germany) equipped with AXioCam HR.

Fluorescence Activated Cell Sorting (FACS). BMMs were seeded in 6-well plates at a density of 5×10^5 cells per well and incubated for 24 h. BMMs were grown to approximately 60% confluency in 6-well plates and then incubated with nanoparticles for 4 h. After the cells were washed twice with PBS and trypsinized for 3 min, the cells were harvested and washed twice with PBS. The cells were fixed by paraformaldehyde aqueous solution (2.0%) and analyzed by flow cytometry (FACS Calibur: BD Biosciences, San Jose, CA, USA). The excitation wavelength was set at 488 nm.

Cytotoxicity Assay. After treating the BMMs with nanoparticles for indicated time periods (12 h, 24 h, 36 h, and 48 h), they were stained with propidium iodide (Sigma) and then analyzed by a flow cytometer. The excitation wavelength was 488 nm.

RESULTS AND DISCUSSION

Synthesis. In order to enhance the cellular uptake of the oligopeptides model drug into the BMMs, two series of dendritic molecules with amine or guanidinium groups were synthesized as shown in Figure 1. SF-A1 was synthesized by ring-opening polymerization of N-carboxy anhydrides of DL-Phe on the stearylamine. The degree of polymerization was about 3 by ¹H NMR spectrum. The SF-A2 was synthesized by the condensation reaction between carboxylic acid of α,ϵ -dibutyloxycarbonyl-lysine and amino group of SF-A1 by using EDC and NHS as coupling agents. After the deprotection of the butyloxycarbonyl groups of SF-A2 by trifluoroacetic acid (TFA), SF-A2 with dendritic amine groups was prepared. The repetition of the same procedure gave dendritic SF-A4 with four amino groups.

To synthesize the SF-G1 with guanidinium groups, amino group of SF-A1 was coupled with carboxylic acid of 4-guanidinobutyric acid (GBA) using EDC and NHS as coupling agents. SF-G2 and SF-G4 were synthesized from SF-A2 and SF-A4, respectively, by a similar coupling method. ¹H NMR, IR analysis, and MALDI-TOF mass spectra confirmed the structure of SF-A1–SF-A4 and SF-G1–SF-G4. In ¹H NMR spectra, the methylene peak of the stearyl group at 1.2–1.4 ppm, methylene peak of the lysine group at 1.7–1.8 ppm, and methylene peak of the 4-guanidinobutyric group at 3.2 ppm confirm the progress of the reaction (Supporting Information Figure S1a) (15, 16). IR spectra of the SF-G1, SF-G2, and SF-G4 showed stronger peaks at 1649 cm^{-1} and 1555 cm^{-1} corresponding to the stretching vibration of C=N and bending vibration of N–H, respectively (Supporting Information Figure S1b). The wide band at 3400 cm^{-1} corresponds to the stretching vibration of N–H group. The strong peaks at 1649, 1555, and 1380 cm^{-1} suggested that the guanidinylation had been successful (17). MALDI-TOF mass spectra confirm the molecular ion peaks for the products as indicated in the experimental section.

Particle Analysis. During preparation of the FITC-IILAVY loaded nanoparticles, the stearyl moieties act as the hydrophobic core of the nanoparticles, whereas the amine groups or guanidinium groups with positive charges are located on the surface of the nanoparticles. The poorly water-soluble FITC-IILAVY was encapsulated into the polymeric nanoparticles due to preferential partitioning of the drug by hydrophobic interactions. The effective hydrodynamic size and zeta potential of FITC-IILAVY loaded nanoparticles were estimated by using a

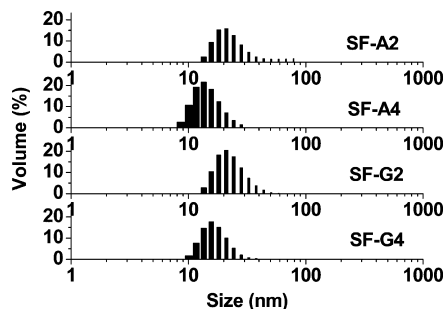


Figure 2. Apparent size of SF-A2, SF-A4, SF-G2, and SF-G4 in water determined by dynamic light scattering study.

Table 1. Zeta-Potential of the Carriers in Water

carrier	SF-A1	SF-A2	SF-A4	SF-G1	SF-G2	SF-G4
ζ potential (mV)	44 ± 3	54 ± 4	55 ± 1	52 ± 1	67 ± 1	85 ± 2

Zetasizer. SF-A1 and SF-G1 formed nanoparticles with a wide range of 40–2000 nm and 50–500 nm, respectively, whereas SF-A2, SF-A4, SF-G2, and SF-G4 formed nanoparticles with a narrow range of 10–45 nm (Figure 2). The encapsulation efficiency of the drug was 17–18% for SF-A2, SF-A4, SF-G2, and SF-G4, resulting in the formation of nanoparticles with a drug loading content of 0.45–0.55%. The drug encapsulated nanoparticles were dialyzed using cellulose membrane (MWCO 3500 Da) in an excess amount of water for 24 h during which some fraction of the drug might be released out of the membrane, thus decreasing the encapsulation efficiency. When the number of amine or guanidinium groups in the carrier increased, size and size distribution of nanoparticles slightly decreased. Zeta potential determines the surface charge of nanoparticles. A high value of zeta potential indicates a high surface charge of the nanoparticles, which leads to strong repellent interactions among the nanoparticles in dispersion and thus can give high stability to the nanoparticle in water. All nanoparticles prepared from SF-A1–SF-A4 and SF-G1–SF-G4 showed positive zeta potential in the range (44 ± 3)–(85 ± 2) mV and good stability in water (Table 1). The zeta potentials of the nanoparticles steadily increased as the number of amine groups or guanidinium groups increased. In addition, guanidinium modified carriers showed larger zeta potential than amine modified carriers.

Cellular Uptake. Oligoarginine works as a cell penetrating peptide and the effectiveness of cell penetration of oligoarginine-conjugated protein (GCN 4) increased as the number of arginine repeating units increased (10). Our system used the stearyl group and oligophenylalanine as a hydrophobic block, where the drug encapsulated nanoparticles are coated with guanidinium groups by a self-assembly process. The cellular uptake of nanoparticles containing FITC-IILAVY was investigated for SF-G4 and SF-A4 as a function of time. The fluorescence intensity increased with time (1 h, 1.5 h, 2 h, 3 h, 4 h) (Figure 3a). Two points can be emphasized for our system. First, FACS analysis showed that guanidinium groups modified nanoparticles (SF-G4) showed excellent penetration into the BMMs. The oligoarginine with four repeating units (R_4) was reported to be ineffective as CPP (10). However, current SF-G4 with four guanidinium groups in a molecule showed excellent translocation ability. This behavior comes from the self-assembly of the SF-G4 with hydrophobic blocks of stearyl-oligophenylalanine and hydrophilic blocks (G_4). On a nanoparticle, the guanidinium groups are located on the surface of the nanoparticle and exhibit a polyarginine-like behavior. Second, guanidinium groups modified nanoparticles (SF-G4) were significantly more effective in

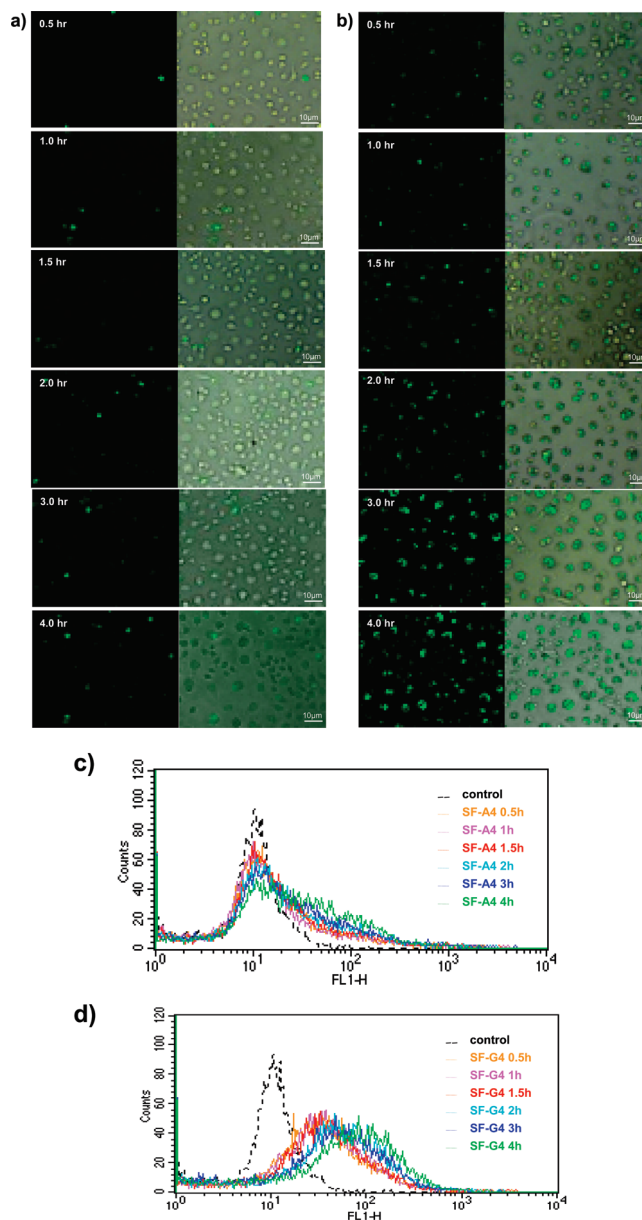


Figure 3. Intracellular delivery of oligopeptides into BMMs. Fluorescence images of internalized oligopeptides by SF-A4 (a) and SF-G4 (b). Both fluorescence images (left) and fluorescence/transmission overlapped images (right) are shown. The scale bars in (a) and (b) are 10 μ m. Flow cytometric histograms of internalized oligopeptides by SF-A4 (c) and SF-G4 (d). Control experiment of the model drug is carried out in the absence of carriers.

penetrating into the BMMs than amino group modified nanoparticles (SF-A4). The detailed mechanism of the difference is under investigation. Previous study by Harashima et al. reported that the octaarginine/DNA complex showed higher transfection efficiency than octalysine/DNA complex (18). They suggested that the enhanced transfection of octaarginine/DNA complex comes from the different mode of endosomal escape from the late endosome with low pH. In our system, the model neutral oligopeptide drug was encapsulated in the guanidinium group coated nanoparticle. In addition, the enhanced translocation of the nanoparticle is observed more in the guanidinium group coated nanoparticle than the amino group coated nanoparticle. The favorable hydrogen bonding interactions between guanidinium groups with dispersed positive charges and negative residues of the phospholipids present on the cell surface might be responsible for such behavior (19, 20). Kinetic study also

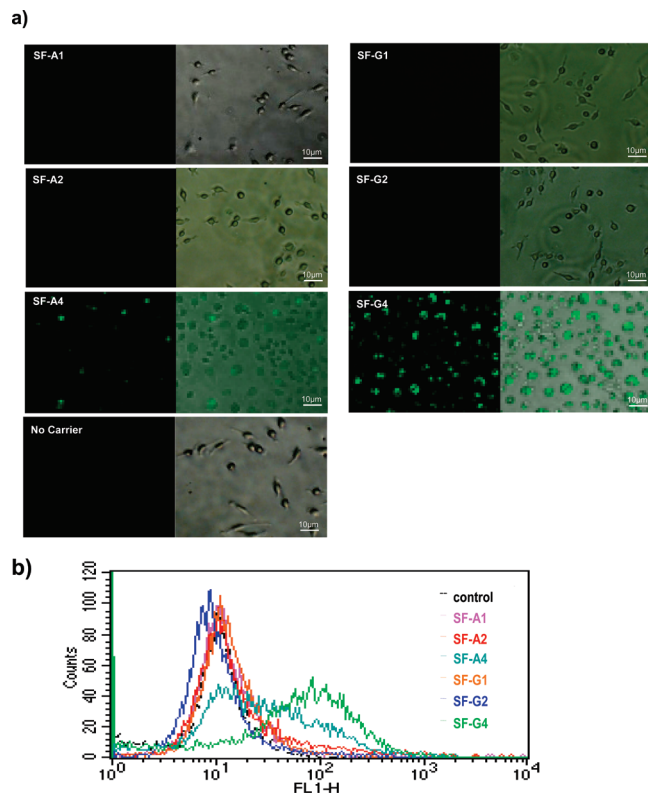


Figure 4. Comparison of carriers for internalization of oligopeptides into BMMs in 4 h. (a) Fluorescence images of internalized oligopeptides by the functionalized carriers. Control experiment of the oligopeptides is carried out in the absence of carriers. The scale bar is 10 μm . Both fluorescence images (left) and fluorescence/transmission overlapped images (right) are shown. (b) Flow cytometric histograms of internalized oligopeptides by the functionalized carriers.

suggested that 4 h is sufficient for the penetration study of the nanoparticles for comparative purposes with other nanoparticles of SF-A1–SF-A4 and SF-G1–SF-G4.

To compare the penetration of the FITC-IILAVY loaded nanoparticles into the BMMs, BMMs were incubated with nanoparticles for 4 h. Fluorescence image and FACS analysis suggested that the SF-G4 system most efficiently penetrates into the cells (Figure 4). Many variables affect the uptake property of nanoparticles, including adhesion to the cell surface, size, and surface charge of the nanoparticle, and so forth. On the basis of current results, we can speculate that the mechanisms of internalization of nanoparticles through the cell membrane may be endocytosis, where the positive charge of the nanoparticles interacts with the negative charge of the phospholipid membrane. SF-G4 nanoparticles possess higher density of guanidinium group than SF-G1 and SF-G2. The higher uptake of SF-G4 by BMM cells is caused by the high positive charge of the nanoparticles as shown by a large ζ -potential. The fact that SF-G4 showed higher translocation ability than SF-A4 also supports previous suggestion that the guanidinium groups have favorable interactions with negatively charged functional groups in the cell membrane (19, 20). The resulting ion pairs have the capability of translocation across the cell membrane.

Cytotoxicity Assay. A drug delivery system should possess biocompatibility or cytocompatibility, as well as a delivery function. HIV-Tat (48–60) was reported to show a 90% cell survival rate at 100 μM for HeLa cells and mouse macrophage RAW264.7 (10, 21). We investigated the FACS plot of BMMs after incubation for 48 h with SF-A4 and SF-G4 in the polymer solution 100 $\mu\text{g}/\text{mL}$ (62 μM for SF-G4 and 91 μM for SF-A4) in culture medium, respectively (Figure 5). PLL (M_w 15 000–

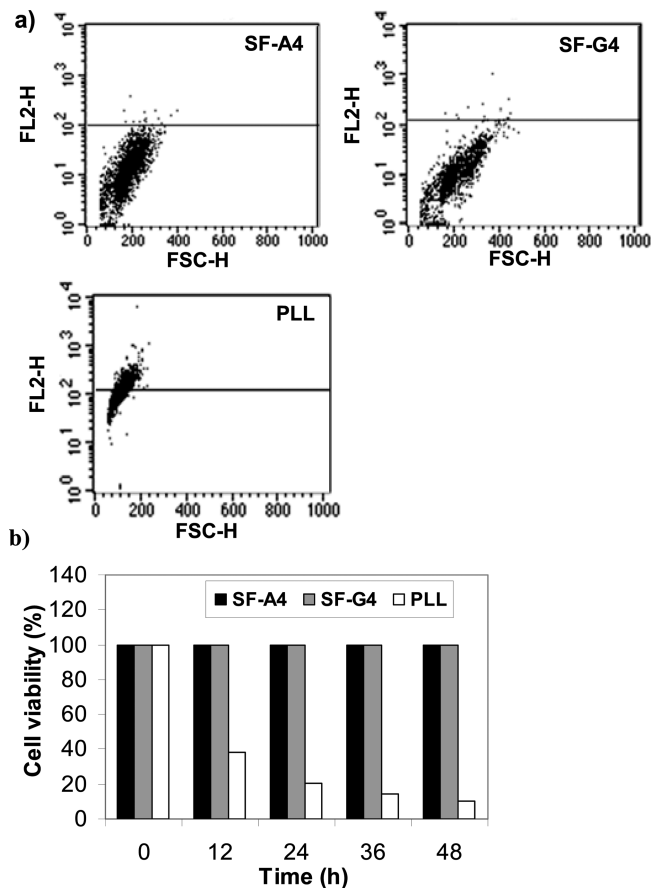


Figure 5. Cytotoxicity of carriers for BMMs. (a) FACS plot of BMMs in 48 h of incubation. (b) Cell viability in the polymer solution (100 $\mu\text{g}/\text{mL}$ in culture medium) for 48 h. Poly(L-lysine) ($M_w = 15\,000\text{--}30\,000$ Da) was used for control.

30 000) was used as a negative control in this research. SF-A4 and SF-G4 in a concentration of 100 $\mu\text{g}/\text{mL}$ did not show cytotoxicity, whereas more than 80% of the BMMs incubated with PLL died.

To conclude, dendritic molecules with amine and guanidinium groups were synthesized and their nanoparticles containing FITC labeled model oligopeptide drug (FITC-IILAVY) were prepared. FACS and spectrofluorimetry analysis showed that (1) the efficiency of intracellular delivery increased by increasing the number of the positive charged groups and (2) the nanoparticles functionalized with dendritic guanidinium groups demonstrated better ability to cross the BMM membranes than amino groups. The carriers (SF-A4 and SF-G4) did not exhibit any significant cytotoxicity against BMMs. Current research suggests that SF-G4 with hydrophobic block and four hydrophilic guanidinium groups is a promising drug delivery carrier for peptide drug targeting osteoclast precursors.

ACKNOWLEDGMENT

This work was supported by the Midcareer Researcher Program through NRF grant funded by the MEST (2007-0055790/2009-0080447) and Korea Science and Engineering Foundation (KOSEF) National Research Laboratory (NRL) Program grant funded by the Korean government (MEST) (R0A-2008-000-20001-0).

Supporting Information Available: ¹H NMR and FTIR of all carriers (SF-A1–SF-A4, SF-G1–SF-G4) are provided. This material is free of charge via the Internet at <http://pubs.acs.org>.

LITERATURE CITED

- (1) Zaidi, M. (2007) Skeletal remodeling in health and disease. *Nat. Med.* *13*, 791–801.
- (2) Teitelbaum, S. L. (2000) Bone resorption by osteoclast. *Science* *289*, 1504–1508.
- (3) Greig, I. R., Idris, A. I., Ralston, S. H., and Hof, R. J. V. (2006) Development and characterization of biphenyl sulfonamides as novel inhibitors of bone resorption. *J. Med. Chem.* *49*, 7487–7492.
- (4) Kim, H., Choi, H. K., Shin, J. H., Kim, K. H., Huh, J. Y., Lee, S. A., Ko, C. Y., Kim, H. S., Shin, H. I., Lee, H. J., Jeong, D., Kim, N., Choi, Y., and Lee, S. Y. (2009) Selective inhibition of RANK blocks osteoclast maturation and function and prevents bone loss in mice. *J. Clin. Invest.* *119*, 813–825.
- (5) Vladimir, P. T. (2008) Cell-penetrating peptide-modified pharmaceutical nanocarriers for intracellular drug and gene delivery. *Pept. Sci.* *90*, 604–610.
- (6) Lindgren, M., Hallbrink, M., Prochiantz, A., and Langel, U. (2000) Cell-penetrating peptides. *Trends Pharmacol. Sci.* *21*, 99–103.
- (7) Futaki, S. (2005) Membrane-permeable arginine-rich peptides and the translocation mechanisms. *Adv. Drug Delivery Rev.* *57*, 547–558.
- (8) Wender, P. A., Mitchell, D. J., Pattabiraman, K., Pelkey, E. T., Steinman, L., and Rothbard, J. B. (2000) The design, synthesis, and evaluation of molecules that enable or enhance cellular uptake: Peptoid molecular transporters. *Proc. Natl. Acad. Sci. U.S.A.* *97*, 13003–13008.
- (9) Futaki, S., Goto, S., and Sugiura, Y. (2003) Membrane permeability commonly shared among arginine-rich peptides. *J. Mol. Recogn.* *16*, 260–264.
- (10) Futaki, S., Suzuki, T., Ohashi, W., Yagami, T., Tanaka, S., Ueda, K., and Sugiura, Y. (2001) Arginine-rich peptides: An abundant source of membrane-permeable peptides having potential as carriers for intracellular protein delivery. *J. Biol. Chem.* *276*, 5836–5840.
- (11) Wender, P. A., Galliher, W. C., Goun, E. A., Jones, L. R., and Pillow, T. H. (2008) The design of guanidinium-rich transporters and their internalization mechanisms. *Adv. Drug Delivery Rev.* *60*, 452–472.
- (12) Jeong, Y., Joo, M. K., Bahk, K. H., Choi, Y. Y., Kim, H. T., Kim, W. K., Lee, H. J., Sohn, Y. S., and Jeong, B. (2009) Enzymatically degradable temperature-sensitive polypeptide as a new in-situ gelling biomaterial. *J. Controlled Release* *137*, 25–30.
- (13) Montserrat, D. F., Dolores, F. F., Montserrat, M., Victor, S., Hamish, R., Miriam, R., and Fernando, A. (2005) Combinatorial approaches towards the discovery of new tryptase inhibitors. *Bioorg. Med. Chem. Lett.* *15*, 1659–1664.
- (14) Carolina, G. G., Nicolas, T., Madeleine, B., Amelie, B., and Elias, F. (2007) Encapsulation of dexamethasone into biodegradable polymeric nanoparticles. *Int. J. Pharm.* *331*, 153–159.
- (15) Martin, A. L., Bernas, L. M., Rutt, B. K., Foster, P. J., and Gillies, E. R. (2008) Enhanced cell uptake of super paramagnetic iron oxide nanoparticles functionalized with dendritic guanidines. *Bioconjugate Chem.* *19*, 2375–2384.
- (16) Wender, P. A., Kreider, E., Pelkey, E. T., Rothbard, J., and van Deusen, C. L. (2005) Dendrimeric molecular transporters: Synthesis and evaluation of tunable polyguanidino dendrimers that facilitate cellular uptake. *Org. Lett.* *7*, 4815–4818.
- (17) Wessel, H. P. (1993) Synthesis of 6-guanidino-hexoses and 5-guanidino-pentoses. *J. Carbohydr. Chem.* *12*, 1173–1186.
- (18) El-Sayed, A., Khalil, I. A., Kogure, K., Futaki, S., and Harashima, H. (2008) Octaarginine-and octalysine-modified nanoparticles have different modes of endosomal escape. *J. Biol. Chem.* *283*, 23450–23461.
- (19) Rothbard, J. B., Jessop, T. C., Lewis, R. S., Murray, B. A., and Wender, P. A. (2004) Role of membrane potential and hydrogen bonding in the mechanism of translocation of guanidinium-rich peptides into cells. *J. Am. Chem. Soc.* *126*, 9506–9507.
- (20) Rothbard, J. B., Jessop, T. C., and Wender, P. A. (2005) Adaptive translocation: the role of hydrogen bonding and membrane potential in the uptake of guanidinium-rich transporters into cells. *Adv. Drug Delivery Rev.* *57*, 495–504.
- (21) Futaki, S., Nakase, I., Suzuki, T., Zhang, Y., and Sugiura, Y. (2002) Translocation of branched-chain arginine peptides through cell membranes: flexibility in the spatial disposition of positive charges in membrane-permeable peptides. *Biochemistry* *42*, 7925–7930.

BC100066K